Scanning Microscopy

Volume 5 | Number 4 Article 20

11-8-1991

Correlation of Cochlear Pathology with Auditory Brainstem and Cortical Responses in Cats with High Frequency Hearing Loss

R. J. Mount
Hospital for Sick Children, Toronto

R. V. Harrison
Hospital for Sick Children, Toronto

S. G. Stanton
University of Toronto

A. Nagasawa
Hospital for Sick Children, Toronto

Scanning Microscopy, Vol. 5, No. 4, 1991 (Pages 1105-1113) 0891-7035/91$3.00+.00
Scanning Microscopy International, Chicago (AMF O'Hare), IL 60666 USA

CORRELATION OF COCHLEAR PATHOLOGY WITH AUDITORY BRAINSTEM AND CORTICAL RESPONSES IN CATS WITH HIGH FREQUENCY HEARING LOSS

R.J. Mount[1*], R.V. Harrison[1,2,3], S.G. Stanton[3] and A. Nagasawa[1]

[1]Department of Otolaryngology and the Research Institute, Hospital for Sick Children, Toronto, Ontario
Departments of [2]Otolaryngology and [3]Physiology, University of Toronto, Toronto, Ontario

(Received for publication August 5, 1991, and in revised form November 8, 1991)

Abstract

Newborn kittens were treated with the aminoglycoside amikacin to produce a bilateral high frequency cochlear hearing loss. The degree and stability of hearing loss were confirmed by recording auditory brainstem evoked potentials (ABR audiograms). After maturation, cochleotopic frequency representation within primary auditory cortex (AI) was mapped using standard microelectrode recording techniques. The cochlear sensory epithelium was assessed with SEM and the pattern of damage compared with the ABR audiograms and cortical frequency maps.

Amikacin treatment resulted in various patterns of haircell damage towards the base of the cochlea. A relatively abrupt transition between damaged and undamaged haircell regions resulted in an ABR audiogram with normal threshold to low frequencies and a high frequency elevation with a steep cut-off slope. In the cortical map, low frequency representation was normal, but anterior areas contained only neurons tuned to a common frequency which corresponded to the frequency-place position of the boundary of the haircell lesion and to the cut-off frequency of the audiogram. A large transitional zone of the cochlear lesion correlated with a gradual cut-off slope to the audiogram and again a remapping of the anterior and normally high frequency area to a common lower frequency. Haircell loss or damage (i.e. disarray of stereocilia) in lower frequency regions of the cochlea correlated with a significant reorganization of the lower frequency bands in the cortical map.

We conclude from this study that the pattern of cochleotopic organization of the cortex is dependent on the pattern of activity in the ascending sensory pathway during early stages of development.

KEY WORDS: Cochlear pathology, auditory cortex, hearing, inner ear, ototoxic drugs, cortical plasticity, cat, scanning electron microscopy.

*Address for correspondence:
R.J. Mount, Dept. of Otolaryngology,
Hospital for Sick Children, 555 University Ave.,
Toronto, Canada M5G 1X8 Phone No. (416) 598-6551

Introduction

The aim of this study is to see if long term alteration to the functional state of the cochlear sensory epithelium results in organizational changes to auditory cortex.

Previous studies, mainly in other sensory systems, indicate that integrity of the sensory input during neonatal development is essential for normal cortical representation. For example Wiesel and Hubel (1974) showed abnormal development of visual cortex in animals with deprived visual input from birth. In the somatosensory system, an abnormal sensory map of body surface results from digit removal or deinnervation in early development (Merzenich and Kaas, 1982).

We hypothesize that the development of cochleotopic organization in primary auditory cortex will be modified by a selective lesion of the haircells of the cochlea. To reliably produce a basal cochlear lesion we used the ototoxic antibiotic amikacin. Such aminoglycosides are known to produce lesions to the sensory cells of the cochlea preferentially in the high frequency, basal region (Hawkins and Lurie, 1953; Lim, 1976; Hunter-Duvar and Mount, 1978; Harrison and Evans, 1979). Although the outer haircells are damaged first, in the long term, adjacent inner haircells are also affected. We used this tool to create a basal cochlear lesion in neonatal cats within a few days of birth.

Part of our goal was to model human sensorineural hearing loss from birth. We therefore chose the kitten because it is an altricious animal in which the functional and morphological development of the hearing system is somewhat incomplete at birth. Although the neonatal kitten is not at an exactly equivalent development stage to the human newborn, we suppose that neonatal hearing loss in our model is approximately analogous to congenital or neonatal hearing loss in humans.

The cat was also an ideal experimental animal because primary auditory cortex (AI) is situated on the surface of the medial temporal gyrus making it readily available for electrophysiological recording experiments. Within AI, neurons are normally arranged in tonotopic, or more correctly, cochleotopic, bands. Posteriorly, neurons reflect activity from the apical

region of the cochlea, and respond best to low stimulus frequencies; anteriorly neurons reflect activity of basal cochlear regions, i.e. are tuned to high frequencies (Woolsey and Walzl, 1942; Rose, 1949; Woolsey and Van der Loos, 1970; Merzenich, et al., 1975; Imig and Adrian, 1977; Reale and Imig, 1980).

In the present study, we have found that abnormal cochleotopic maps in AI resulted from neonatal cochlear lesions. It appears that the cortical representation of cochlear areas is critically dependent on the integrity of the cochlear sensory epithelium. We present here a correlation between: (a) the pattern of cochlear haircell damage as demonstrated by SEM, (b) measures of the ascending activity as indicated by auditory brainstem evoked responses (ABR), and (c) the abnormal cortical cochleotopic maps measured from AI.

Material And Methods

This study involved the following steps:

a) Production of cochlear lesions in neonatal animals (animal model of neonatal high frequency cochlear hearing loss)

b) Confirmation of the pattern of cochlear hearing loss using auditory brainstem evoked potential (ABR) audiometry.

c) Electrophysiological mapping of cochleotopic organization in primary auditory cortex.

d) Characterization of cochlear haircell damage using SEM.

These experimental methods are outlined below.

Animal Model

Newborn kittens were treated with amikacin (400mg/kg/day s.c.) for four days beginning at postnatal day one. Pilot studies had indicated that this regime produces bilateral lesions to the high frequency regions of the cochleas. Cortical mapping and cochlear SEM evaluations were carried out in these animals at maturity (12 - 18 months).

Evoked Potential Measure of Audiometric Thresholds

The functional status of the peripheral auditory system was determined by measuring auditory brainstem response (ABR) audiograms (ABR threshold responses to tone pip stimuli). During recording sessions, animals were lightly anaesthetized with ketamine (25 mg/kg i.m.). A vertex-mastoid scalp electrode configuration was used. ABRs were amplified $x10^4$ and bandpass filtered between 30 Hz and 3 kHz. ABRs were realized with 300 averaging sweeps. The stimuli were tone pips between 0.5 and 24 kHz, with 2 ms rise/fall times and a 2 ms plateau, delivered via a free field system. ABR thresholds to tone pips were determined by recording the potentials to a decreasing stimulus intensity series, using 5 dB steps near to threshold. Threshold determinations were based on the most evident ABR waveform (P3 or P4 in the cat). Threshold was designated as being midway between the lowest stimulus level which provided an ABR response, and the 5 dB lower level at which there was no response.

ABR audiograms were determined at four weeks of age to confirm threshold elevations caused by cochlear lesions and at eight and twelve weeks to confirm the stable nature of the lesions. Audiograms were repeated prior to cortical mapping, typically one year later.

In this paper, we chose to present ABR threshold elevations in dB loss relative to normal ABR threshold. Thus in Figures 4 and 9 the ABR audiograms were determined by a comparison of the ABR thresholds in the treated animal with the mean ABR thresholds in eight normal controls determined using an identical stimulation and recording system. We chose this format for ABR threshold representation because it most simply and clearly demonstrates threshold shift, the factor of prime interest in the study. The mean (normalized to 0 dB; analogous to 0 dBHL) and standard deviations of these controls are shown in Figure 1, providing an indication of individual differences between animals and thus the confidence level associated with our 0 dB reference. The precision of other ABR thresholds (shown in Figures 4 and 9) should be interpreted accordingly. ABR waveforms are not presented in this paper; some treated animals exhibited unusual waveforms, and these data will be published separately.

Cortical Mapping

Cortical frequency maps were derived during acute 48 - 60 hour electrophysiological recording sessions in the anaesthetized animal (sodium pentobarbital and ketamine hydrochloride, approximately 0.5 and 0.75 mg/kg/hour i.v. respectively). Salient methods were as follows: The temporal surface was exposed, photographed and the activity of single neurons or small unit clusters was recorded in response to contralateral acoustic stimulation.

Spike activity was recorded using tungsten microelectrodes (1-4 Mohm) at depths of 0-600 μm from the cortical surface. The acoustic stimuli were presented through a hollow ear bar inserted into the cut down external meatus. Neuron responses were recorded to tones (10 ms rise/fall; 70 ms plateau) over a wide range of frequencies and intensities delivered in a pseudo-random fashion under computer control. Our acoustic transducers allowed presentation of stimuli up to 50 kHz. Neural spike responses were isolated with a voltage window discriminator and these event times were logged by input to a D/D intelligent interface (Cambridge Electronic Design 1401) hosted by a PC80286 computer. Further details are provided in Harrison et al. (1991). Characteristic frequency (CF) of each unit was determined and plotted on the photograph of the cortical surface according to its location.

Cochlear Morphology

After cortical mapping was completed the animal was deeply anaesthetized (sodium pentabarbital), the thoracic cavity opened and cardiac

perfusion made with room temperature physiological saline. When the perfusate was clear, fixation was commenced with a mixture of 1% paraformaldehyde and 1.25% glutaraldehyde in 0.1 M phosphate buffer, pH 7.4, at room temperature followed by phosphate buffered (pH 7.4) 10% sucrose at 4°C. The skull was removed and the brain and temporal bones dissected out. The brain was further processed as part of a concurrent study.

The cochlea was exposed, the round and oval windows opened and the perilymphatic scalae perfused with fixative. After fixation for a total of two hours, the cochleae were washed overnight in 0.1M phosphate buffer (pH 7.4) then post fixed in buffered 1% OsO_4, all at 4°C. Following dehydration to 70% ethanol, the cochleas were dissected to expose the organ of Corti. After complete dehydration through absolute ethanol, the specimen was critical point dried from CO_2, sputter coated with gold and examined on a JEOL JSM 840 scanning electron microscope at 12 - 20 keV.

In order to associate morphological observations of the cochlea with functional properties (ABR threshold, cortical frequency map) we have used the cochlear place-frequency map based on behavioral threshold changes in cats with cochlear lesions according to Schuknecht (1960). This map is very similar to a more recent map from Liberman (1982) derived from HRP labelling of single cochlear afferents.

Results

Our aim is to compare the morphological status of the cochlear sensory epithelium with ABR audiograms and cortical frequency maps in cats with neonatal basal cochlear damage (high frequency hearing loss). From a total of ten amikacin treated animals we present here the full data from two subjects, our data from a normal animal is typical of the controls we have investigated (N=8).

Normal Control Cats

Scanning EM allows us to view the haircells at the reticular surface of the organ of Corti. As shown in Figure 3, the sensory epithelium of the normal adult cat consists of three rows of outer haircells and one row of inner haircells. Haircells have ordered, upright stereocilia and few if any haircells are missing.

Figure 1 is the mean normalized ABR audiogram from eight control animals. Figure 2 shows the typical cortical map from a normal cat. The primary auditory cortical area (AI) is located on the temporal gyrus, lateral to the sylvian fissure (SF) and approximately bounded by the anterior and posterior ectosylvian fissures (AEF; PEF). Within AI sound frequencies are represented in an orderly fashion reflecting the frequency-place coding within the cochlea (cochleotopic organization). Thus, neurons responding best to low frequency, receiving input from the cochlear apex, are located posteriorly; those activated best by high frequency, deriving input from the base of the cochlea, are positioned anteriorly. Further anterior to the AI boundary is the "anterior field", a secondary

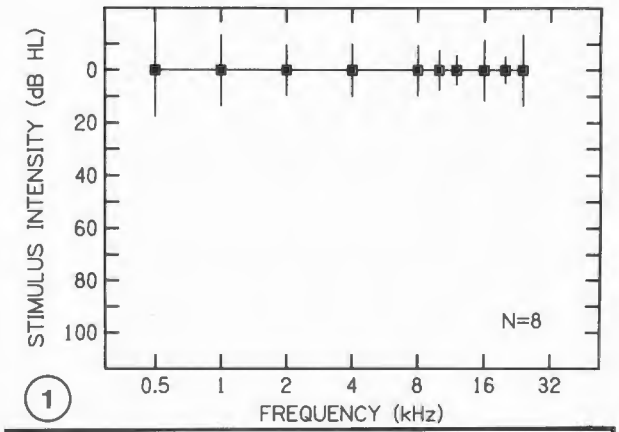

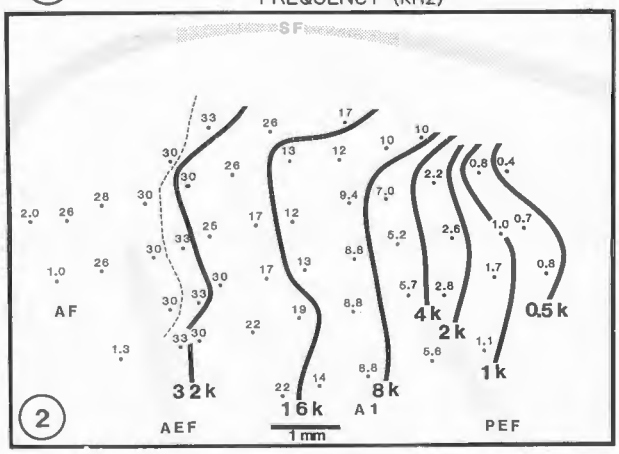

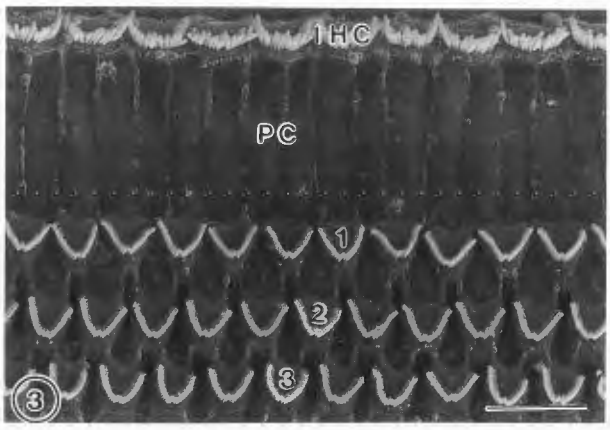

Fig. 1. Mean ABR audiogram from normal adult cats (N=8), normalized to 0 dB (analogous to 0 dBHL). Error bars ± 1 S.D.

Fig. 2. Map of auditory cortex (AI) indicating frequency representation in a normal cat. Dotted line approximates the boundary between primary cortex (AI) and the anterior field (AF). AEF, anterior ectosylvian fissure; PEF, posterior ectosylvian fissure; SF, sylvian fissure.

Fig. 3. Sensory cells of the normal organ of Corti in adult cat. IHC, inner haircells; PC, pillar cells; 1-2-3, first, second and third row outer haircells; bar = 10 μm

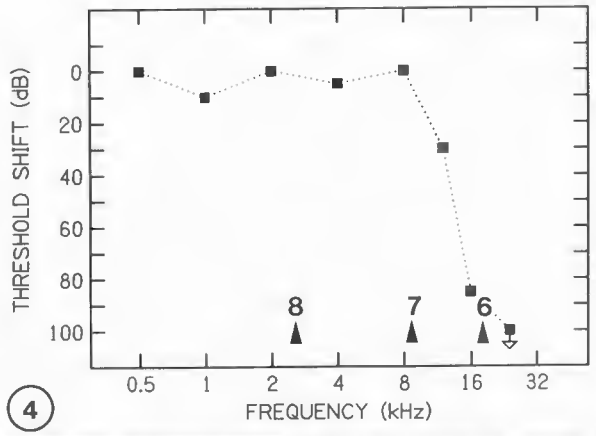

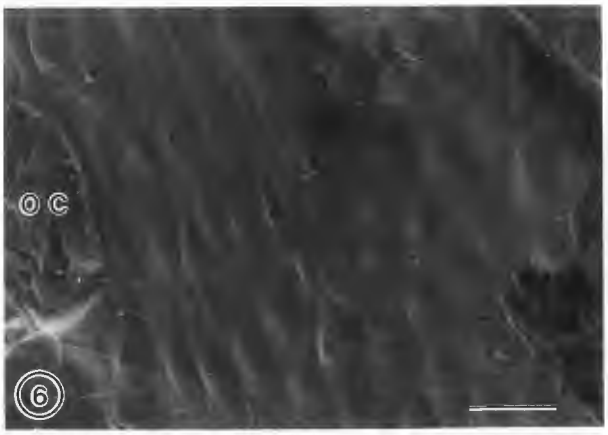

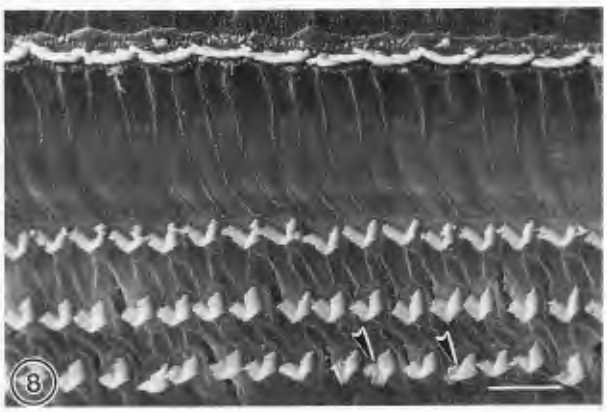

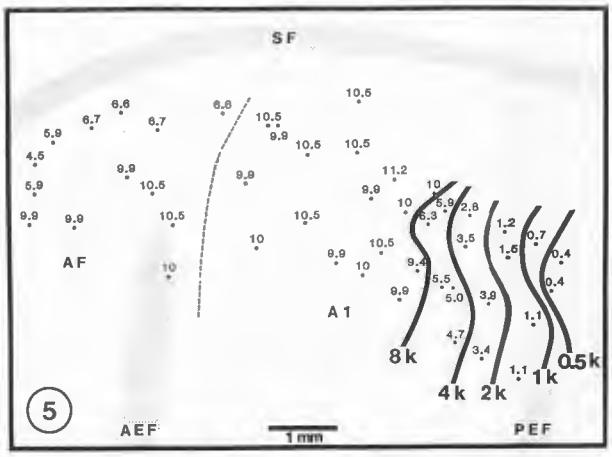

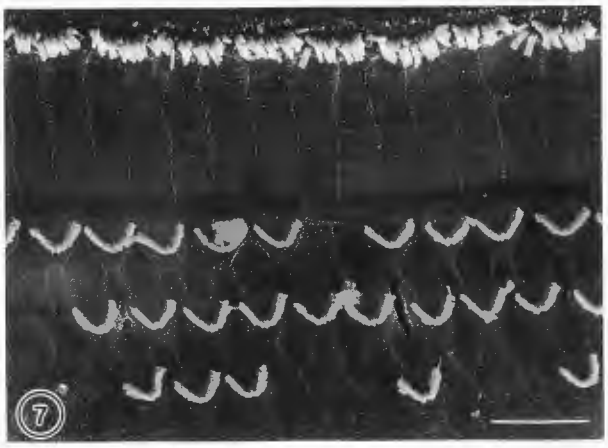

auditory region with a reversed cochleotopic organization.

Although there is some variation from animal to animal in the position and dimensions of AI, Figure 3 and the above general description are typical. Here, in essence, we have a normal sensory epithelium (normal neonatal development), a normal activation of the peripheral auditory pathways, and therefore a normal cortical frequency map.

Treated Animals (Neonatal hearing loss)

Figures 4 - 15 describe our results from two treated animals. For each cat we show the ABR audiogram (Figs. 4 & 9) and the cortical frequency map (Figs. 5 & 10) together with examples of cochlear

Fig. 4. ABR audiogram of amikacin treated animal JL23. Arrows indicate approximate frequency-place position of figs. 6 - 8.

Fig. 5. Cortical map of amikacin treated animal JL23. Units responding best to frequencies below 8 kHz have a normal distribution; no high frequency representation was present. Dotted line approximates the boundary between primary cortex (AI) and the anterior field (AF). AEF, anterior ectosylvian fissure; PEF, posterior ectosylvian fissure; SF, sylvian fissure.

Fig. 6. Typical basal portion of cochlea from an amikacin treated animal. The structure of the organ of Corti is missing and replaced with an epithelial cell layer. OC, possible remnant of organ of Corti. Bar = 25 μm

Fig. 7. Lower basal turn (8 kHz region) of amikacin treated animal JL23 showing scattered loss of outer haircells. Bar = 10 μm

Fig. 8. Upper basal turn (3 kHz region) of animal JL23. All haircells are present, however there is some damage to stereocilia (arrows). Bar = 10 μm

damage. In animals treated with amikacin over a short time course the basal portion of the cochlea is totally denuded of sensory receptors. More apical regions typically contain a normal complement of haircells. Between these two extremes exists a range of damage which varies from animal to animal. Third row outer haircells are normally damaged first followed by those in the second and then the first row. Inner haircells are the least susceptible to amikacin induced damage, often appearing undamaged over long lengths of cochlea in which outer haircells are totally absent. The pattern of outer haircell damage is variable and can sometimes occur in a reverse order with the first row being most damaged followed by the second and then third rows (see Figs. 7 & 14).

In our first experimental animal, the amikacin treatment has resulted in a threshold elevation starting at c. 8 kHz. This is reflected in the ABR audiogram of figure 4. Note the very steep cut-off slope in the audiogram above 8 kHz (>80 dB/octave). The cortical map indicates a near normal distribution of neurons with low characteristic frequencies (< 8 kHz) and iso-frequency contours similar to those of normal controls (e.g. fig. 2). The remainder of the field, normally containing neurons responding best to increasingly higher frequencies, is taken up by units with a characteristic frequency of 10 kHz. This frequency corresponds to both the high frequency cut-off slope of the ABR audiogram, and to the border of the damaged region in the cochlea. Figures 6 to 8 show example regions of the cochlear sensory epithelium about this border area.

The basal portion of the cochlea is totally denuded of haircells as in all our amikacin treated animals. Often all supporting cells of the organ of Corti have also degenerated as shown in Figure 6. Figure 7 shows scattered haircell damage in the lower basal turn. This damage decreases towards the basal/middle turn boundary where a full haircell complement is present, although some damage to stereocilia persists (see, for example, arrows in Fig. 8). The area of transition from total haircell loss to scattered loss occurs in the 8 - 12 kHz frequency region of the cochlea.

The ABR audiogram and cortical map of our second treated cat are shown in Figures 9 and 10. The audiogram indicates a high frequency cut-off having a gradual slope beginning in the low frequencies at approximately 1 kHz with a total loss at about 16 kHz and above. The frequency region over which there is threshold change is approximately 4 octaves. In AI cortex, the majority of the field contains neurons responding best to an input of 6 - 7 kHz. Lower frequencies are not represented as ordered iso-frequency bands, some frequencies are not represented at all, others are poorly represented by islands of cells.

The large 6 - 7 kHz area of the cortical map (Fig. 10) corresponds to the most basal cochlear region in which there are some remaining (inner) haircells. Damage in this region is illustrated by Figure 11. The damage in the cochlea is not simply progressive from this point. Progressing apically we find a region of total damage (Fig. 12). Then, further apically, we observe another area of scattered surviving inner haircells, but with some fusion of stereocilia (Fig. 13). Outer haircells begin to return in the upper basal/lower middle turns (the 1 - 2 kHz region). There, inner haircells are mainly present, but stereocilia are disarrayed and in some instances fused (Fig. 14). In the lower middle turn (1 kHz frequency region), there is a full complement of haircells although stereociliar damage exists (Fig. 15).

Discussion

Sensory areas of the cortex are known to exhibit extensive organizational changes (plasticity) as a result of deprivation or unusual patterns of sensory input from an early age. This has been shown, for example, in the visual cortex (Wiesel and Hubel, 1963, 1974; Movshon and Van Sluyters, 1981), in the cortical representation of rat whiskers (Waite and Taylor, 1978) and in somatosensory cortex (Merzenich and Kaas, 1982; Merzenich et al. 1983; Kaas et al. 1983). For example, early deprivation of somatosensory input by removal of whiskers or digits amputation results in a remapping of associated sensory cortical areas. Regions unused because of lack of input are utilized for coding of areas of adjacent sensory epithelium e.g. input from whiskers or digits bordering the lesion. A conceptually similar finding was observed by Robertson and Irvine (1989) who reported changes to frequency mapping in auditory cortex after unilateral, punctate cochlear lesions in adult animals. These authors noted that neurons, in cortical areas corresponding to the frequency region of the cochlear lesion, were tuned to the characteristic frequency of neurons arising from the the border of the cochlear lesion. Our study differs in many respects from that of Robertson and Irvine, however we report here a similar finding.

A very prevalent type of sensory disorder in humans is cochlear hearing loss in which, basal regions of the cochlea are damaged giving rise to a high frequency deafness. Often, such deficits are present at birth or arise during infancy, resulting in a chronically abnormal pattern of sensory input to auditory cortex. This is the situation that we have specifically modelled in this study, by inducing, in neonatal kittens, haircell damage in the basal region of the cochlea using the ototoxic aminoglycoside amikacin. This drug treatment resulted in bilateral and symmetrical haircell damage. We assume that humans with congenital cochlear hearing loss will have cortical configurations which have been altered to a degree similar to those that we have demonstrated here.

Our study differs significantly from that of Robertson and Irvine (1989) because we have specifically modelled neonatal sensorineural hearing loss. Nevertheless, both studies point to a similar finding of an "expansion" of cortical frequency representation. Our findings differ in relation to the extent of the expanded region. In the guinea pigs of Robertson and Irvine's study, 0.7 mm is reported to be the maximum extent of reorganization (≈ 18% of AI

field length). In our study, we have observed iso-frequency expanded areas extending up to 4 mm in the rostro-caudal dimension (≈ 50% of AI field length).

Critical in these studies of cortical frequency mapping is the method for evaluation of the characteristic frequencies of unit responses. In our study, we have objectively and systematically mapped neural response areas and had relatively little difficulty in assigning a CF value to units. In all cases, CF was defined as the frequency of the most sharply tuned tip to the excitatory area of the response curve. In abnormal shaped curves, e.g. "W" shaped frequency threshold curves (FTCs), we chose the highest frequency tip, even if it had a threshold more elevated than the tail region. This was a reasonable strategy based on our knowledge of changes to tuning curves at the cochlear fibre level, in various conditions of pathology. For further details of FTCs in these animals see Harrison et al. (1991).

In both of our treated animals, the tuning curves corresponding to the border region were abnormal, having a "W" shape. The general shape of tuning curves in the expanded cortical region was similar to that in the border units. Thus we judge the neurons in the expanded areas to have a common input from neurons arising at the border of damage in the cochlea. Although we observe these functional changes in the cortical maps we have no idea, at present, at what level in the auditory pathways this reorganization takes place.

The aim of this report is to make some correlation between the abnormal cortical maps and the cochlear lesions from which they are ultimately caused. Using SEM techniques we have been able to characterize the degree and extent of cochlear haircell damage in our animal models. When we correlate this pattern of cochlear damage to the abnormal cortical frequency representation, it is clear that the latter is critically dependant on the pattern of excitatory input from the sensory epithelium of the cochlea. Two factors are most noteworthy.

Firstly, cortical regions that appear to be remapped are those with no normal sensory input, i.e. they correspond to cochlear frequency areas with total haircell degeneration. Neurons within such areas reflect activity from inputs arising from the border of the cochlear lesion, between total haircell loss and a surviving haircell population. In areas with uneven, scattered patterns of damage the most influential area appears to be the most basal border. For example, in the data shown in Figures 4 - 8 the border area immediately basal to the photomicrograph of Figure 7 corresponds to the 10 kHz expanded frequency region.

Secondly, cochlear areas with scattered haircell loss or more subtle damage give rise to reduced ascending input, and this appears to prevent the development of a normal cortical representation (in terms of AI surface area or normal iso-frequency bands) as illustrated in Figures 9 - 15. In the 1 - 4 kHz frequency region, there is scattered haircell damage as shown by Figures 14 and 15. Note that haircells may be present but with stereocilia disarray, or cells may be absent. In any case, we assume that the total activity arising from this cochlear area is much less than normal. These frequency regions are very poorly represented in AI. It is of interest to note that although such representation is reduced, the audiogram shows relatively normal thresholds. We suggest that this reflects some sensory redundancy, relatively few normal threshold units are required to provide ABR threshold information.

We note in this paper two clear ways in which the pattern of damage to the sensory epithelium, and thus sensory input, determines the development of frequency representation in central auditory areas. More precise correlation between degree of haircell pathology and cortical maps will be the subject of further studies.

The reorganization observed may not arise entirely at the cortical level. It is possible, indeed highly likely, that such changes reflect the cumulative result of a series of smaller reorganizations both at cortex and at lower levels in the system, perhaps starting at the midbrain (inferior colliculus) or brainstem level (e.g. cochlear nucleus). We are presently attempting to determine whether this is the case.

Our interpretation that expanded iso-frequency regions reflects a reorganization of the adult map is still tentative. There are a number of alternative possibilities. It is possible that the observed organization is a "retention of an immature tonotopic map" (Garraghty & Schwaber, personal communication). Our data does not allow us to comment further on this because we have carried out no assessments in developing neonates.

Fig. 9. ABR audiogram of amikacin treated animal JL30. Arrows indicate approximate frequency-place position of figs. 11 - 15.

Fig. 10. Cortical map of animal JL30. Most of AI appears to be devoted to units responding to 6-7 kHz tones. Legend same as Figure 5.

Fig. 11. One of several scattered inner haircells remaining in the lower basal turn (6 - 8 kHz region) of animal JL30 . Bar = 5 μm

Fig. 12. Lower basal turn (6 kHz region) area of animal JL30. No haircells and only a minimal organ of Corti structure are present. PC, pillar cell; bar = 10 μm

Fig. 13. Upper basal turn (3 kHz region) of animal JL30. Showing damaged inner haircell. Bar = 5 μm

Fig. 14. Upper basal turn of animal JL30, (2 kHz region). Many outer and inner haircells are present but haircell and stereociliar damage is prevalent. Bar = 10 μm

Fig. 15. Lower middle turn of animal JL30, (1 kHz region) showing that all haircells are present, but many stereocilia are disarrayed. Bar = 10 μm

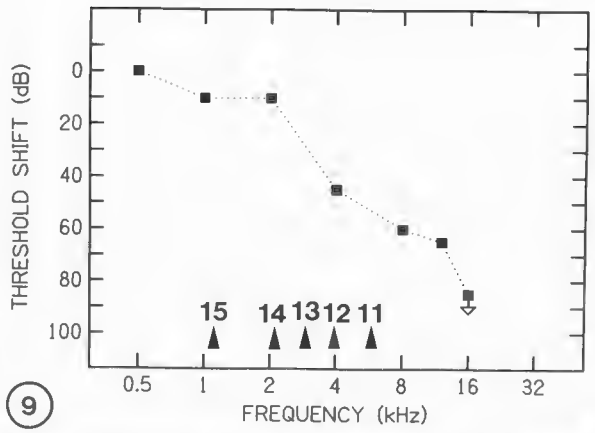

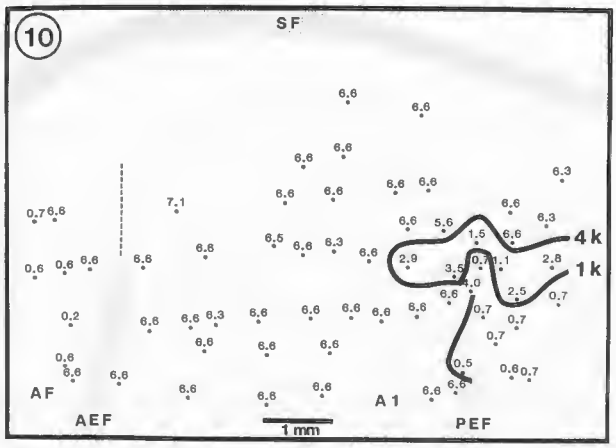

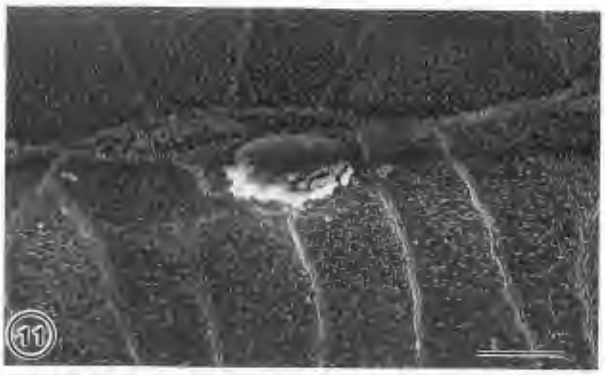

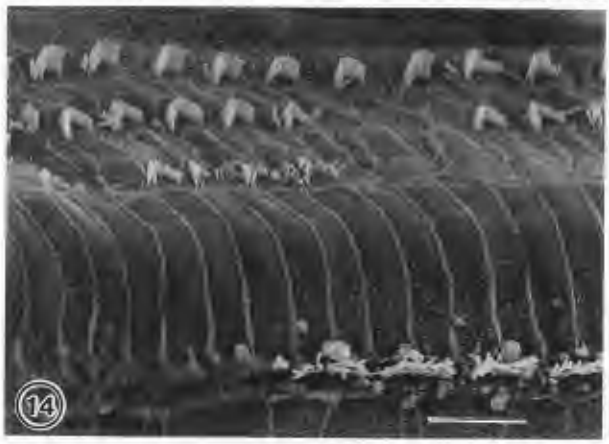

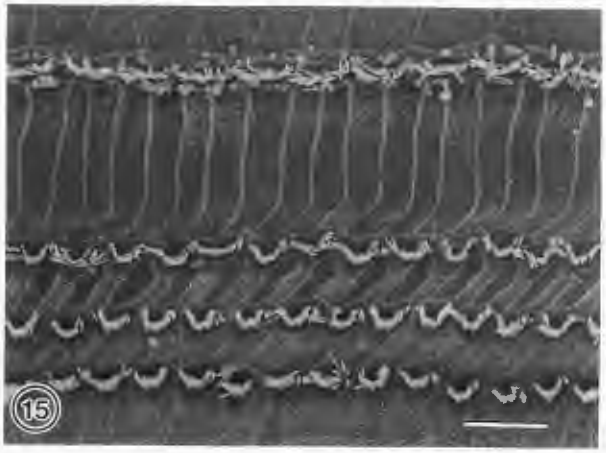

Acknowledgments

This research was supported by grants from MRC (Canada) and with generous support from the Masonic Foundation of Ontario.

References

Harrison RV and Evans EF (1979) Cochlear fibre responses in guinea pigs with well defined cochlear lesions. Scand. Audiol. Suppl. 9: 83-92.

Harrison RV, Nagasawa A, Smith DW, Stanton SG and Mount RJ (1991) Reorganization of auditory cortex after neonatal high frequency cochlear hearing loss. Hear. Res., 54: 11-19

Hawkins JE Jr and Lurie MH. (1953) The ototoxicity of dihydrostreptomycin and neomycin in the cat. Ann Otol Rhinol Laryngol, 62: 1128-1148

Hunter-Duvar IM and Mount RJ. (1978) The organ of Corti following ototoxic antibiotic treatment. Scanning Electron Microsc., 1978;II: 423-430

Imig T and Adrian HO. (1977) Binaural columns in the primary field (AI) of cat auditory cortex. Brain Res. 138: 241-256.

Kaas JH, Merzenich MM and Killackey HP. (1983) The reorganization of somatosensory cortex following peripheral nerve damage in adult and developing mammals. In: W.M. Cowen (ed.) Annu. Rev. Neurosci. 6, Palo Alto CA, 325-356.

Lim DJ. (1976) Ultrastructural cochlear changes following acoustic hyperstimulation and ototoxicity. Ann Otol Rhinol Laryngol, 85: 740-751.

Liberman MC. (1982) The cochlear frequency map for the cat: Labeling auditory-nerve fibers of known frequency. J. Acoust. Soc. Am. 72: 1141-1149

Merzenich MM and Kaas JH. (1982) Reorganization of mammalian somatosensory cortex following peripheral nerve injury. Trends Neurosci. 434-436.

Merzenich MM, Kaas JH, Wall J, Nelson RJ, Sur M and Felleman DJ. (1983) Topographic re-organization of somatosensory cortical areas 3B and 1 in adult monkeys following restricted deafferentation. Neuroscience, 8: 33-35.

Merzenich MM, Knight PL and Roth GL. (1975) Representation of the cochlea within primary auditory cortex in the cat. J. Neurophysiol., 38: 231-249.

Movshon JA and Van Sluyters RC. (1981) Visual neural development. Ann. Rev. Psychol., 32: 477-522.

Reale RA and Imig TJ. (1980) Tonotopic organization in auditory cortex of the cat. J. Comp. Neurol., 192: 265-291.

Robertson D and Irvine DRF. (1989) Plasticity of frequency organization in auditory cortex of guinea pigs with partial unilateral deafness. J. Comp. Neurol., 282: 456-471.

Rose JE. (1949) The cellular structure of the auditory area of the cat. J. Comp Neurol., 91: 409-439.

Schuknecht HF. (1960) Neuroanatomical correlates of auditory sensitivity and pitch discrimination in the cat. In: Rasmussen GL and Windle WF (ed). Neural Mechanisms of the Auditory and Vestibular Systems. Charles C Thomas, Illinois, USA., 76-92

Waite PMS and Taylor PK. (1978) Removal of whiskers in young rats causes functional changes in cerebral cortex. Nature., 274: 600-602.

Wiesel TN and Hubel DH. (1963) Single cell responses in striate cortex of kittens deprived of vision in one eye. J. Neurophysiol., 26: 1003-1017.

Wiesel TN and Hubel DH. (1974) Ordered arrangement of orientation columns in monkeys lacking visual experience. J. Comp. Neurol., 158: 307-318.

Woolsey CN and Walzl EM. (1942) Topical projection of nerve fibers from local regions of the cochlea to the cerebral cortex of the cat. Johns Hopk. Hosp. Bull., 71: 315-344.

Woolsey TA and Van der Loos H. (1970) The structural organization of layer IV in the somatosensory region (SI) of mouse cerebral cortex. Brain Res, 17: 205-242

Discussion with Reviewers

W.W. Clark: What is the length of the newborn kitten cochlea? Can the frequency-place map for adult cats be superimposed on the newborn cochlea?

Authors: Although the kittens are being treated neonatally all our anatomical observations and cortical mapping are made in the adult animal. We have no direct experience measuring the newborn cochlea, however we think it unlikely that it would differ significantly from the length of the adult.

W.W. Clark: How can one rule out the possibility that the units located in "high frequency" regions but responding to frequencies near the edge of the cochlear lesion were always present but with high thresholds, and were not detected?

Authors: In our control (normal) animals, we have observed a strict cochleotopic organization of neurons such that in any region of the cortex (AI) all neurons appear to have a similar CF (although their tuning properties may be different). This applies to units with a range of minimum thresholds. In addition we have conducted a control study in which cochlear function above 4 kHz was acutely attenuated (TTS by acoustic trauma). This temporarily removed input to high frequency areas of AI arising from the basal cochlear areas. Under these circumstances we could not record any neuron activity in the high frequency cortical area. We conclude that in anterior areas there are normally few, if any, neurons that are tuned to lower frequencies.

S. Rydmarker: You say haircell damage is variable concerning which haircell row is the first to be damaged. Following noise exposure or endolymphatic hydrops the "direction" of the damage process is more consistent. Do you have an explanation for the difference?

Authors: We have no precise explanation for the for the difference. The order and degree of damage resulting from aminoglycosides is both time and dose dependent, see for example Lenoir and Puel (1987), Hear. Res. 26: 199-209.

S. Rydmarker: Would you expect the same kind of cortical disorganization following noise exposure of an adult human?

Authors: Our data do not give a direct answer. However based on data from the somatosensory system,

where limited cortical reorganization has been noted in the adult animal (dynamic alterability; Merzenich et al., 1983), we suppose that some changes will occur in adults after an acquire hearing loss. We might expect similar expanded regions corresponding to the high frequency cut-off slope of the audiogram, but such expansion would be confined in extent to $\approx$ 500 μm. This is based on the concept that such expansion is mediated by local cortical neural interactions; neural arborizations tend to be about 500-700um.

P.E. Garraghty and M.K. Schwaber: Is it possible to extract from these data a heuristic hypothesis as to the relative functions of inner and outer haircells?
Authors: No.

R.J. Salvi: A conventional cochleogram done with light microscopy would have provided a comprehensive description of the degree of haircell loss along the length of the cochlea. Is your SEM technique reliable enough to make hair cell counts over the entire cochlea in order to construct a cochleogram?
Authors: While it is possible to assess haircells over large regions of the cochlea with SEM, it is very difficult to do a total assessment in either the hook region or lesion areas. Ideally one would like to obtain a full count of present and absent haircells as well as a total assessment of haircell integrity. In our preliminary studies we have chosen to limit our observations to SEM assessment of cochlear damage (including stereociliar integrity) at points of interest along the cochlear length. This is adequate for cochleas with a classical basal lesion and relatively normal apical regions. We agree that in some cases, especially a cochlea with a complex pattern of damage along much of its length, a cochleogram will be of value. We intend to make such analyses in the future as required.

R.J. Salvi: How did the response areas or tuning curves of cortical units in amikacin treated ears differ from those in normal ears?
Authors: Responses from low frequency (posterior) cortical regions, receiving input from undamaged cochlear areas are similar to those of normal animals. The tuning curves of cortical neurons receiving input from areas of cochlear damage had a range of shapes similar to those reported by others in pathological cochlear nerve studies. Thus, thresholds were elevated, and commonly the tuning curve had a "w' shape. More information and examples of FTCs are to be found in Harrison et al. 1991.

R.J. Salvi: The CFs of units in the auditory nerve have been reported to shift downward in frequency as a result of cochlear damage. Could the over-representation of low CF units in the cortex be due to a downward shift in CF arising in the periphery or is it a central effect?
Authors: The over-representation of low CF units is not caused by a downward shift in CF in the remaining units. If this were the case, tuning curve shapes would be different according to their proximity to the region corresponding to the peripheral lesion. In fact, the shapes of the FTCs in units in the expanded region were similar to each other, perhaps indicating that their inputs have a common source

R.J. Salvi: When does the human cochlea reach maturity? How does this compare with the cat?
Authors: This is an important question for all those working with animal models of human development. There is no simple answer. In terms of the CAP reaching a normal latency and amplitude, the human cochlea appears to be mature at 4 - 6 weeks. In the kitten, cochlear fibre FTCs are of normal threshold and tuning by days 20 - 30 (Romand, R. Neuroscience Lett., 35, 271-276). In these terms, there appears to be a reasonable parallel between the two mammalian species.